Nanoparticle-Based Metamaterials as Multiband Plasmonic Resonator Antennas

Arif E. Çetin, Mustafa Turkmen, *Member, IEEE*, Serap Aksu, and Hatice Altug, *Member, IEEE*

***Abstract*—Plasmonic metamaterials based on metal-dielectric nanostructures exhibit unique optical properties such as high near-field enhancement, negative refractive indexing, and optical cloaking. In this paper, we present a plasmonic multiband metamaterial based on UT shaped nanoparticles. In order to understand the multispectral response, we analyze the near-field distributions at the corresponding resonance frequencies. In addition, we both numerically and experimentally, show the dependence of the spectral response on the geometrical parameters of the structure. By embedding the system in a dielectric cladding medium, we show strong sensitivities of the resonant behavior to the refractive index and thickness of the dielectric load. Due to its tunable multiband spectral characteristics, the proposed metamaterial antenna can be used for wide range of applications, such as wavelength-tunable active filters, optical modulators, ultrafast switching devices, and biosensing.**

***Index Terms*—Metamaterials, nanofabrication, optical communications, optical filters, plasmonics, resonators, subwavelength optics.**

I. Introduction

METAMATERIALS have received tremendous interests over the past few years due to their unusual electromagnetic properties. These properties provide unique applications, i.e., negative indexing, extraordinary near field enhancement, high-frequency magnetism, superlens, electromagnetic cloaking, and nonlinear optics [1]–[17]. Metamaterials are artificially fabricated subwavelength materials with optical and electromagnetic characteristics depending on their microscopic structure and geometry. Latest advances in the field of nanofabrication technology have enabled the realization of metamaterials in different sizes and shapes. In recent years, metamaterials based on metallic nanostructures have received significant attention as they can concentrate and manipulate light at subwavelength range through surface plasmons (SPs) that are collective oscillations of free electrons in a metal [18], [19]. These nanostructures can also be termed as plasmonic resonator antennas (PRA) due to their analogy to the conventional microwave antennas [20]. These metamaterials based on PRAs can offer wide tunability of spectral responses [21]–[24]. Furthermore, as SPs enhance the sensitivity to the surface conditions, these structures are employed in biosensing and surface enhanced spectroscopy [25]–[32].

In this paper, we propose a nanoparticle-based plasmonic metamaterial composed of individual U- and T-shaped PRAs as shown in Fig. 1. We investigate the spectral response of these PRAs both numerically and experimentally. The proposed metamaterial supports a multiband spectral response. In addition, its design has a compact geometry. Moreover, the spectral response of the system has dual- or triple-bands with respect to the polarization direction of the illumination source. To understand this behavior, we analyze the structure by the 3 dimensional-finite difference time domain (3D-FDTD) method [33] and obtain the corresponding near-field distributions. We experimentally determine the spectral dependence on the geometrical parameters for controlling the resonance frequencies. We then embed the resonator system into a dielectric medium to realize a multiresonant dielectric loaded metamaterial antenna. We determine the sensitivity of the structure to the refractive index and thickness

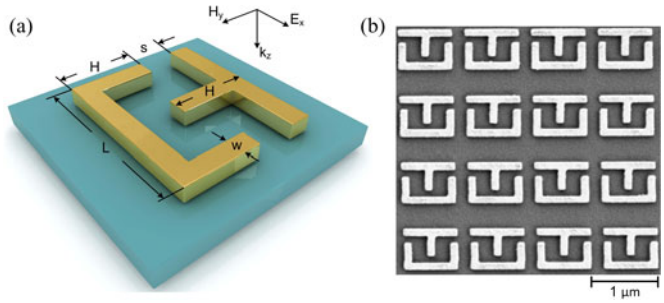

Fig. 1. (a) Schematic view of UT-shaped metamaterial antenna. In figure, the polarization and propagation direction of the incident wave is included. (b) SEM image of the fabricated structure with corresponding parameters: $H = 400$ nm, $L = 800$ nm, $s = 100$ nm, and $w = 100$ nm.

Manuscript received June 27, 2011; accepted October 19, 2011. Date of publication November 15, 2011; date of current version January 11, 2012. This work was supported by the National Science Foundation (NSF) CAREER Award ECCS-0954790, ONR Young Investigator Award 11PR00755-00-P00001, Massachusetts Life Science Center New Investigator Award, NSF Engineering Research Center on Smart Lighting EEC-0812056, and also by DOD/Army Research Laboratory under Grant W911NF-06-2-0040. The work of M. Turkmen was supported by The Scientific and Technological Research Council of Turkey (TUBITAK). A. E. Çetin and M. Turkmen contributed equally to this work. The review of this paper was arranged by Associate Editor G. Ramanath.

A. E. Çetin is with the Department of Electrical and Computer Engineering, Boston University, Boston, MA 02215 USA and also with Photonics Center, Boston University, Boston, MA 02215 USA (e-mail: acetin@bu.edu).

M. Turkmen is with the Department of Electrical and Computer Engineering, Boston University, Boston, MA 02215 USA, Photonics Center, Boston University, Boston, MA 02215 USA, and also with the Department of Electrical and Electronics Engineering, Erciyes University, Kayseri 38039, Turkey (e-mail: turkmen@bu.edu).

S. Aksu is with the Division of Materials Science and Engineering, Boston University, Boston, MA 02215 USA and also with Photonics Center, Boston University, Boston, MA 02215 USA (e-mail: saksu@bu.edu).

H. Altug is with the Department of Electrical and Computer Engineering, Boston University, Boston, MA 02215 USA, the Division of Materials Science and Engineering, Boston University, Boston, MA 02215 USA, and also with Photonics Center, Boston University, Boston, MA, 02215, USA (e-mail: altug@bu.edu).

Color versions of one or more of the figures in this paper are available online at http://ieeexplore.ieee.org.

Digital Object Identifier 10.1109/TNANO.2011.2174160

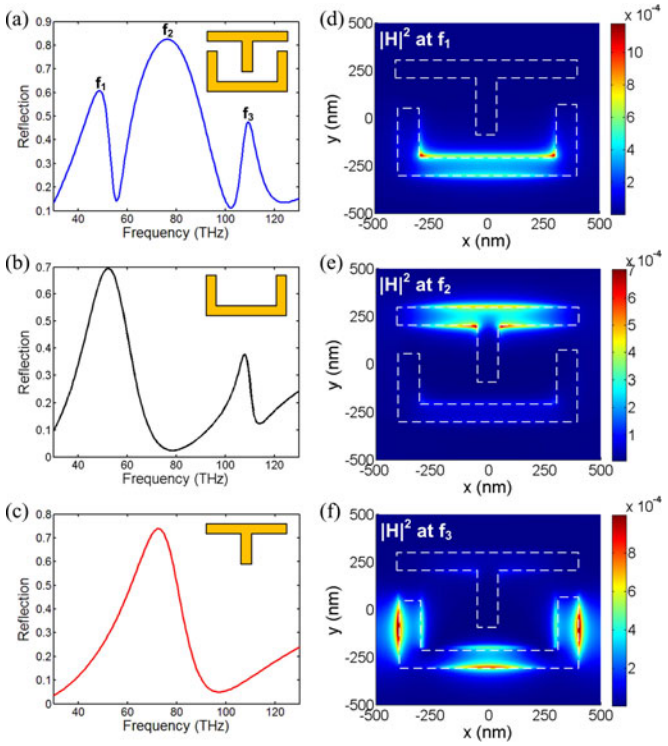

Fig. 2. Reflection spectra of (a) UT-, (b) U-, and (c) T-shaped PRAs. In (d)–(f), field distributions (total magnetic field intensity, $|H|^2$) are shown for UT-shaped antenna at three different resonance peaks: f_1, f_2, and f_3. The corresponding parameters are: $H = 400$ nm, $L = 800$ nm, $s = 100$ nm, and $w = 100$ nm.

of the cladding medium for fine-tuning of the resonances. Due to the tunability of the multiband spectral response, such PRAs can be used for wide range of applications, i.e., wavelength-tunable active filters, optical modulators, ultrafast switching devices, and biosensing.

II. Numerical Analysis

Fig. 1 shows the schematic view of the UT-shaped PRA design. In the figure, the geometrical parameters are L the length of the structure, H the height, w the rod width, and s the distance between the individual U- and T-shaped nanorods. Here, the structure stands on a silicon nitride (SiN_x) substrate with refractive index of 2.16. For the numerical analysis, the structure is modeled by the 3D-FDTD method. The unit cell of the system consists of two individual elements, U- and T-shaped gold nanoparticles. Along x and y axes, periodic boundary condition is used and along $\pm$z, which also corresponds to the direction of the illumination source, perfectly matched layer is used. The frequency-dependent dielectric constants of the metals are taken from [34].

In far field, for y-polarized illumination source incident from air, the system supports a dual-band spectral response while for x-polarized illumination source, it provides a triple-band response. In this study, we focus on the x-polarized incident source case. In order to understand the physical origin of the multispectral response, we look at the field distributions corresponding to the three distinct resonance peaks as shown in Fig. 2(a) (f_1, f_2, and f_3). Fig. 2(d)–(f) show the total magnetic

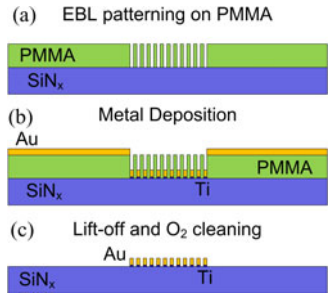

Fig. 3. Fabrication process steps: (a) EBL is performed on the PMMA-coated surface and EBL performed patterns are removed by MIBK–IPA solution. (b) PMMA layer is covered with 5-nm-thick titanium and 30-nm-thick gold. (c) Lift-off process is performed to get rid of the gold, covering the unexposed surfaces. Then, plasma cleaning is performed to remove the remaining PMMA on the surface.

field intensities $|H|^2$ at the air–metal interface (top surface of the nanoparticles) for the corresponding reflection peaks. The first- and third-order modes of the UT-shaped antenna are originated from the individual U-shaped antenna while the second mode is originated from the individual T-shaped one as shown in Fig. 2(b) and (c), respectively. For the first-order mode of the UT-shaped antenna at f_1, the field enhancement is mainly localized at the inner edges of the bottom horizontal bar [see Fig. 2(d)]. For the second-order mode at f_2, it is focused at the center of the top horizontal bar [see Fig. 2(e)]. For the third-order mode at f_3, it is localized at right and left vertical rods and the center of the bottom horizontal bar [see Fig. 2(f)]. Furthermore, these field enhancements are maximum at the top surface of the structure (air–metal interface). This is highly desirable for biosensing applications as it increases the overlap between the electromagnetic fields of the SPs and the analytes in the surrounding medium [30], [31].

III. Fabrication of the UT-Shaped Metamaterial Antennas

For the experimental demonstration of the multiresonant characteristic, the proposed UT-shaped PRAs are fabricated on a SiN_x film. The fabrication process is summarized in Fig. 3. We first perform electron-beam lithography (EBL) on a resist polymethyl methacrylate (PMMA)-coated film. Then, EBL-defined patterns are removed by a methyl isobutyl ketone–isopropyl alcohol (MIBK–IPA) solution. The EBL-exposed parts are then covered with 5-nm-thick titanium (adhesion layer) and 30-nm-thick gold layers. Later, lift-off process is performed to get rid of the gold layers covering the unexposed surfaces. Finally, plasma cleaning is performed to remove the rest of the resist on the surface [35]. SEM images given in Fig. 1(b) clearly show that the surface of the fabricated structures is smooth, and nanorods are well defined. The unit cells are observed to be uniform over large areas.

Fabricated structures are characterized optically by a Fourier transform infrared (FTIR) microscope. Our experimental setup consists of an IR microscope coupled to a Bruker FTIR spectrometer with a KBr splitter. Normally incident electromagnetic radiation, shown in Fig. 1(a), is used to efficiently excite the SP

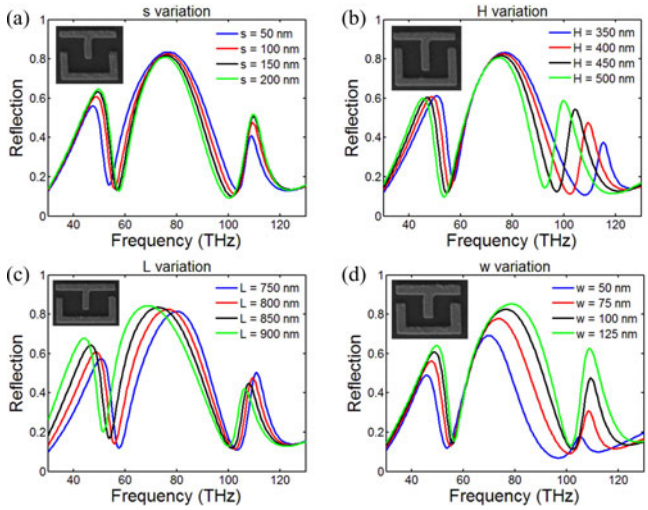

Fig. 4. Spectral response of the UT-shaped antennas with varying geometrical parameters. (a) s-variation at fixed $H = 400$ nm, $L = 800$ nm, and $w = 100$ nm. Subfigure shows the SEM image for s $= 200$ nm case. (b) H-variation at fixed s $= 100$ nm, $L = 800$ nm, and $w = 100$ nm. Subfigure shows the SEM image for $H = 500$ nm case. (c) L-variation at fixed $H = 400$ nm, $s = 100$ nm, and $w = 100$ nm. Subfigure shows the SEM image for $L = 900$-nm case. (d) w-variation at fixed $H = 400$ nm, $L = 800$ nm, and $s = 100$ nm. Subfigure shows the SEM image for $w = 125$-nm case.

modes on the resonators. Reflected IR signal is collected by a Cassagrian reflection optics (NA $= 0.4$) and coupled into a liquid N_2-cooled mercury cadmium telluride detector. Reflection data are normalized using an optically thick gold standard.

IV. Experimental Results for the Spectral Dependence on Geometrical Parameter

It is highly desirable to understand the physical origin of the spectral dependence for determining control mechanisms of the resonant behavior of the structures [36], [37]. Therefore, we experimentally analyze UT-shaped nanoparticles by varying geometrical parameters. We observe that, the multiband behavior of the UT-shaped PRAs show strong dependence on geometry. Fig. 4 shows the change in the spectral response for different s, H, L, and w variations. In Fig. 4(a), s is varied while the other parameters are kept constant: $L = 800$ nm, $H = 400$ nm, and $w = 100$ nm. As s increases, the amplitude of the reflection peaks of the first- and third-order modes increases slightly while the peak of the second mode shows negligible changes. In addition, with increasing s, the resonance frequency of the first- and third-order modes increases whereas for the second-order mode, it remains almost the same. Fig. 4(b) shows the H dependence of the spectral response. Here, other parameters are kept constant at $s = 100$ nm, $L = 800$ nm, and $w = 100$ nm. As H increases, the resonance frequency of the first-order mode decreases weakly while that of the third-order mode strongly decreases. The second-order mode exhibits almost no change. Besides, the amplitude change of the first two modes is negligible while the amplitude of the third-order mode increases significantly with H. For H variation, the change of the resonance frequency is proportional to the field localization at the arms of the U-shaped nanoparticle. For that reason, the third-order mode where the near-field is strongly localized on the arms of U [see Fig. 2(f)] shows strong dependence on H while the first-order mode, which supports relatively weak near-field localization [see Fig. 2(d)], shows smaller changes. Since for the second-order mode, there is no field localization on the arms, H variation weakly affects the resonance frequency of this mode. In contrast, as shown in Fig. 4(c), the resonance frequency of all three modes decreases with L. (For L variation, other geometrical parameters are: $H = 400$ nm, $s = 100$ nm, and $w = 100$ nm). The amplitude of the first-order mode increases, the third-order mode decreases, and second-order mode shows negligible changes with L. For w variation, other geometrical parameters are kept constant as: $H = 400$ nm, $L = 800$ nm, and $s = 100$ nm. With increasing w, the resonance frequency and the amplitude of all three modes increase as shown in Fig. 4(d). This observation indicates that the UT-shaped PRAs show strong dependence on geometrical parameters. Therefore, the resonant locations of the proposed structure can be easily controlled by changing the geometrical parameters.

V. Dielectric Loaded UT-Shaped Metamaterial Antennas

The spectral response of the antennas can be tuned by introducing a cladding medium on the structure [21]–[24], [38], [39]. For that reason, we tune the spectral response of the UT-shaped antenna by loading easily depositable dielectric materials with different refractive indices, such as, magnesium fluoride, $MgFl_2$ ($n = 1.37$), silicon dioxide, SiO_2 ($n = 1.46$), and aluminium oxide, Al_2O_3, ($n = 1.76$). First, the whole antenna system is fully merged into the dielectric load in a way that the thicknesses of the dielectric and the metal layers are equal ($t = 30$ nm). We determine the dependence of the resonance behavior of the UT-shaped metamaterials on the refractive index in Fig. 5(b). We observe that the resonance frequency of all three modes decreases with the refractive index of the dielectric load. We also calculate the refractive index sensitivity of the system, defined as the change in the resonance wavelength with respect to the change in the refractive index of the cladding medium, for third-order mode, $\Delta\lambda/\Delta n = 423$ nm/RIU. We also determine the change in the field distribution (total electric field distribution, $|E|^2$) with respect to different dielectric materials for the third-order mode. For this propose, we use a field monitor located at one of the arm-tips of the U-shaped nanorod [as illustrated in Fig. 5(a)] where total electric field is maximum for the third-order mode. We observe that with different dielectric loads, the near-field distribution does not change but the field enhancement decreases as shown in Fig. 5(c). For surface enhanced spectroscopy applications, large field intensities are critical. Hence, UT-shaped metamaterial, supporting near-field intensity enhancements as large as 600, is an ideal candidate for these applications. We also determine the change in the resonance frequency with respect to the dielectric load thickness. Fig. 5(d) shows the effect of the thickness of the cladding medium on the spectral response for the case of SiO_2. For all three modes, the resonance frequency decreases with increasing the thickness of the dielectric load. For the third-order

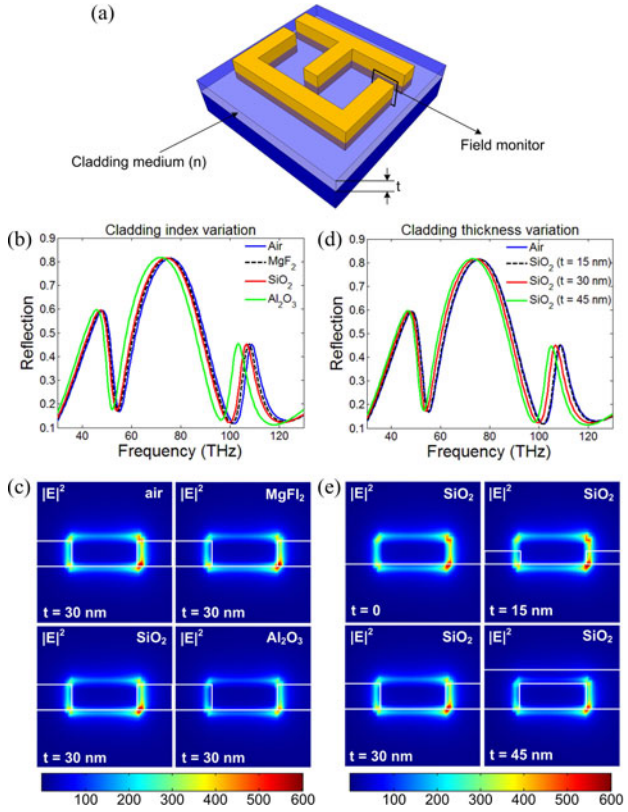

Fig. 5. (a) Schematic view of UT-shaped metamaterial antenna embedded in a dielectric medium with a refractive index n. In figure, the position of the field monitor is illustrated. (b) Reflection spectrum variation of UT-shaped antenna with respect to different dielectric loads, $MgFl_2$ ($n = 1.37$), SiO_2 ($n = 1.46$) and Al_2O_3 ($n = 1.76$). (c) Total electric field distributions for different dielectric loads. (d) Reflection spectrum variation of UT-shaped antenna with respect to different dielectric load thicknesses. Here, the thickness variation is done for SiO_2 and t is varied from 15 to 45 nm. (e) Total electric field distributions for different dielectric load thicknesses. The corresponding parameters are: $H = 400$ nm, $L = 800$ nm, $s = 100$ nm, and $w = 100$ nm.

mode, we observe 4-nm resonance shift with 1-nm load of the cladding medium. This result shows that, the dielectric-loaded plasmonic UT-shaped antennas can be used as an anisotropic metal-dielectric metamaterials with tunable optical properties. We also determine the field distributions of a bare UT-shaped antenna and the one with different dielectric-load thicknesses. Fig. 5(e) shows that the electromagnetic field distributions for different dielectric load thicknesses exhibit the similar behavior with the bare UT-shaped antenna. Therefore, without losing near-field characteristics, we can tune the far-field behavior of the overall metamaterial structure by varying the thickness of the cladding medium.

VI. Conclusion

In this section, we introduce a novel multiresonant metamaterial design based on UT-shaped PRAs. We theoretically show the physical origin of the multiband spectral behavior by field distribution analysis. We experimentally obtain the dependence of the spectral response on geometrical parameters. Embedding the whole structure in a cladding medium, we determine the sensitivities on the refractive index and the thickness of the dielectric medium. In this way, we obtain the control and fine-tuning mechanisms of the spectral behavior of the proposed structure. Such metamaterials with tunable spectral behavior could have far-reaching consequences for chip-based frequency selective optical devices including active filters, optical modulators and biochemical sensors.

References

[1] L. Tong, R. R. Gattass, J. B. Ashcom, S. He, J. Lou, M. Shen, I. Z. Maxwell, J. B. Ashcom, and E. Mazur, "Subwavelength-diameter silica wires for low-loss optical wave guiding," *Nature*, vol. 426, pp. 816–819, 2003.

[2] D. R. Smith, W. J. Padilla, D. C. Vier, S. C. Nemat-Nasser, and S. Schultz, "Composite medium with simultaneously negative permeability and permittivity," *Phys. Rev. Lett.*, vol. 84, p. 4184, 2000.

[3] R. A. Shelby, D. R. Smith, and S. Schultz, "Experimental verification of a negative index of refraction," *Science*, vol. 292, p. 77, 2001.

[4] J. B. Pendry, "Negative refraction makes a perfect lens," *Phys. Rev. Lett.*, vol. 85, p. 3966, 2000.

[5] J. B. Pendry, D. Schurig, and D. R. Smith, "Controlling electromagnetic fields," *Science*, vol. 312, p. 1780, 2006.

[6] V. M. Shalaev, "Optical negative-index metamaterials," *Nat. Photon.*, vol. 1, p. 41, 2007.

[7] N. Engheta, "Circuits with light at nanoscales: Optical nanocircuits inspired by metamaterials," *Science*, vol. 317, pp. 1698–1702, 2007.

[8] A. Ourir, A. Lustrac, and J.-M. Lourtioz, "All-metamaterial-based subwavelength cavities (λ/60) for ultrathin directive antennas," *Appl. Phys. Lett.*, vol. 88, p. 084103, 2006.

[9] M. Turkmen, S. Aksu, A. E. Cetin, A. A. Yanik, and H. Altug, "Multi-resonant metamaterials based on UT-shaped nano-aperture antennna," *Opt. Express*, vol. 19, p. 7921, 2011.

[10] B. Temelkuran, M. Bayindir, E. Ozbay, R. Biswas, M. M. Sigalas, G. Tuttle, and K. M. Ho, "Photonic crystal-based resonant antenna with a very high directivity," *J. Appl. Phys.*, vol. 87, p. 603, 2000.

[11] N. J. Florous, K. Saitoh, and M. Koshiba, "Enhanced thermoplasmonic oscillations in metallic nanostructured particles for the realization of nanofluidic sensors," *IEEE Trans. Nanotechnol.*, vol. 6, no. 5, p. 549, Sep. 2007.

[12] S. M. Sadeghi, "Plasmonic metaresonance nanosensors: Ultrasensitive tunable optical sensors based on nanoparticle molecules," *IEEE Trans. Nanotechnol.*, vol. 10, no. 3, pp. 566–571, May 2011.

[13] B. Joshi, A. Chakrabarty, and W. Qi-Huo, "Numerical studies of metaldi-electricmetal nanoantennas," *IEEE Trans. Nanotechnol.*, vol. 9, no. 6, pp. 701–707, Nov. 2010.

[14] T. J. Yen, W. J. Padilla, N. Fang, D. C. Vier, D. R. Smith, J. B. Pendry, D. N. Basov, and X. Zhang, "Terahertz magnetic response from artificial materials," *Science*, vol. 303, pp. 1494–1496, 2004.

[15] P. Muhlschlegel, H. J. Eisler, O. J. F. Martin, B. Hecht, and D. W. Pohl, "Resonant optical antennas," *Science*, vol. 308, pp. 1607–1609, 2005.

[16] E. Cubukcu and F. Capasso, "Optical nanorod antennas as dispersive one-dimensional FabryPérot resonators for surface plasmons," *Appl. Phys. Lett.*, vol. 95, p. 201101, 2009.

[17] E. Cubukcu, S. Zhang, Y-S. Park, G. Bartal, and X. Zhang, "Split ring resonator sensors for infrared detection of single molecular monolayers," *Appl. Phys. Lett.*, vol. 95, p. 043113, 2009.

[18] A. V. Zayats, I. I. Smolyaninov, and A. A. Maradudin, "Nano-optics of surface plasmon polaritons," *Phys. Rep.*, vol. 408, pp. 131–314, 2005.

[19] S. Lal, S. Link, and N. J. Halas, "Nano-optics from sensing to waveguiding," *Nat. Photon.*, vol. 1, pp. 641–648, 2007.

[20] R. K. Mongia and P. Bhartia, "Dielectric resonator antennas a review and general design relations for resonant frequency and bandwidth," *Int. J. Microw. Millimeter-Wave Eng.*, vol. 4, pp. 230–247, 1994.

[21] W. Dickson, G. A. Wurtz, P. R. Evans, R. J. Pollard, and A. V. Zayats, "Electronically-controlled surface plasmon dispersion and optical transmission through hole arrays in metal films with liquid crystal," *Nano Lett.*, vol. 8, pp. 281–286, 2008.

[22] W. Dickson, G. A. Wurtz, P. Evans, D. O'Connor, R. Atkinson, R. Pollard, and A. V. Zayats, "Dielectric-loaded plasmonic nano-antenna arrays: A metamaterial with tuneable optical properties," *Phys. Rev B*, vol. 76, p. 115411, 2007.

[23] P. R. Evans, G. A. Wurtz, W. R. Hendren, R. Atkinson, W. Dickson, A. V. Zayats, and R. J. Pollard, "Electrically switchable non-reciprocal transmission of plasmonic nanorods with liquid crystal," *Appl. Phys. Lett.*, vol. 91, p. 043101, 2007.

[24] G. A. Wurtz, P. R. Evans, W. Hendren, R. Atkinson, W. Dickson, R. J. Pollard, W. Harrison, C. Bower, and A. V. Zayats, "Molecular plasmonics with tunable exciton-plasmon coupling strength in J-aggregate hybridized Au nanorod assemblies," *Nano Lett*., vol. 7, pp. 1297–1303, 2007.
[25] F. Wang and Y. R. Shen, "General properties of local plasmons in metal nanostructures," *Phys. Rev. Lett*., vol. 97, p. 206806, 2006.
[26] U. Kreibig and M. Vollmer, *Optical Properties of Metal Clusters*. New York: Springer-Verlag, 1995.
[27] H. Xu, E. J. Bjerneld, M. Kall, and L. Borjesson, "Spectroscopy of single hemoglobin molecules by surface enhanced raman scattering," *Phys. Rev. Lett*., vol. 83, pp. 4357–4360, 1999.
[28] J. B. Jackson and N. J. Halas, "Surface-enhanced raman scattering on tunable plasmonic nanoparticle substrates," *Proc. Nat. Acad. Sci*., vol. 101, pp. 17930–17935, 2004.
[29] G. Laurent, N. Felidj, S. Truong, J. Aubard, G. Levi, J. Krenn, A. Hohenau, A. Leitner, and F. Aussenegg, "Imaging surface plasmon of gold nanoparticle arrays by far-field raman scattering," *Nano Lett*., vol. 5, pp. 253–258, 2005.
[30] R. Adato, A. A. Yanik, J. J. Amsden, D. L. Kaplan, F. G. Omenetto, M. K. Hong, S. Erramilli, and H. Altug, "Ultra-sensitive vibrational spectroscopy of protein monolayers with plasmonic nanoantenna arrays," *Proc. Nat. Acad. Sci*., vol. 106, pp. 19227–19232, 2009.
[31] A. E. Cetin, A. A. Yanik, C. Yilmaz, S. Somu, A. Busnaina, and H. Altug, "Monopole antenna arrays for optical trapping, spectroscopy, and sensing," *Appl. Phys. Lett*., vol. 98, p. 111110, 2011.
[32] P. J. Schuck, D. P. Fromm, A. Sundaramurthy, G. S. Kino, and W. E. Moerner, "Improving the mismatch between light and nanoscale objects with gold bowtie nanoantennas," *Phys. Rev. Lett*., vol. 94, pp. 0174021–0174024, 2005.
[33] Finite-difference-time-domain package, Lumerical FDTD Solutions. (2011). [Online]. Available: www.lumerical.com
[34] E. D. Palik, *Handbook of Optical Constants of Solids*. Orlando, FL: Academic, 1985.
[35] S. Aksu, A. A. Yanik, R. Adato, A. Altar, M. Huang, and H. Altug, "High-throughput nanofabrication of plasmonic infrared nanoantenna arrays for vibrational nanospectroscopy," *Nano Lett*., vol. 10, pp. 2511–2518, 2010.
[36] N. Engheta, A. Salandrino, and A. Alu, "Circuit elements at optical frequencies: Nanoinductors, nanocapacitors, and nanoresistors," *Phys. Rev. Lett*., vol. 95, p. 095504, 2005.
[37] M. L. Brongersma, "Plasmonics: Engineering optical nanoantennas," *Nat. Photon*., vol. 2, pp. 270–272, 2008.
[38] B. Maune, R. Lawson, C. Gunn, A. Scherer, and L. Dalton, "Electrically tunable ring resonators incorporating nematic liquid crystals as cladding layers," *Appl. Phys. Lett*., vol. 83, pp. 4698–4691, 2003.
[39] A. E. Cetin and O. E. Mustecaplioglu, "Electrically tunable Dicke effect in double-ring resonator," *Phys. Rev. A*, vol. 81, p. 043812, 2010.

Arif E. Çetin received the B.S. degree in electrical and electronics engineering in 2007 and the M.S. degree in electrical and computer engineering in 2009 both from the Koç University, Istanbul, Turkey. He is currently working toward the Ph.D. degree in the Department of Electrical and Computer Engineering, Boston University (BU), Boston, MA.

Since 2009, he has been with the Laboratory of Integrated Nanophotonics and Biosensing Systems, BU Photonics Center under supervision of Dr. Hatice Altug. His research interests include integrated plasmonic systems for biodetection, plasmonic systems for optical trapping, vibrational spectroscopy, plasmonic metamaterials, computational and experimental electromagnetics, and optics and nanophotonic devices.

Mr. Çetin received Boston University, Photonics Center Junior Fellowship Award in 2009 and The Scientific and Technological Research Council of Turkey Graduate Scholarship in 2007.

Mustafa Turkmen (M'11) received the M.S. and Ph.D. degrees from the Erciyes University, Kayseri, Turkey, both in electrical and electronics engineering, in 2003 and 2009, respectively.

He is an Assistant Professor in the Department of Electrical and Electronics Engineering, Erciyes University. Currently, he is a Visiting Scholar in the Department of Electrical and Computer Engineering, Boston University, Boston, MA. His current research interests include microwave printed circuits, microwave filters, and patch antennas for wireless communication applications, metamaterials, nanoplasmonics, and their applications in chemical and biosensing, and optical communication.

Dr. Turkmen is a recipient of the Graduate and Postdoctoral Research Fellowships from Higher Education Council of Turkey and The Scientific and Technological Research Council of Turkey.

Serap Aksu received the B.S. degree from Sabanci University, Materials Science and Engineering, Istanbul, Turkey, in 2008, with a Chemistry minor. She is currently working toward the Ph.D. degree in the Division of Materials Science and Engineering, Boston University (BU), Boston, MA.

Since 2008, she has been with the Laboratory of Integrated Nanophotonics and Biosensing Systems at BU Photonics Center under supervision of Dr. Hatice Altug. Her current research activities include plasmonics, novel nanofabrication techniques, optical nanoantennas, and their applications in biosensing and vibrational nanospectroscopy.

Hatice Altug (M'10) received the B.S. degree in physics from Bilkent University, Ankara, Turkey, in 2000, and the Ph.D. degree in applied physics from Stanford University, Stanford, CA, in 2007.

She is an Assistant Professor in the Department of Electrical and Computer Engineering, Boston University, Boston, MA, where she is also with the Division of Materials Science and Engineering. Her research interests include integrated nanophotonics, nanoplasmonics, and nanofluidic systems and their application in biosensing, vibrational nanospectroscopy, and optical communication.

Dr. Altug is a recipient of the Presidential Early Career Award for Scientists and Engineers, the Office of Naval Research Young Investigator Award, National Science Foundation CAREER Award, Massachusetts Life Science Center New Investigator Award, IEEE Photonics Society Young Investigator Award, and Boston University College of Engineering Early Career Research Excellence Award. She received the Peter Paul Career Professorship, Intel Graduate Student Fellowship, and IEEE Photonics Society Graduate Student Fellowship. She is the winner of the 2004 Inventors' Challenge competition of Silicon Valley and the 2005 IEEE Photonics Society Best Paper and Research Excellence Award.